GEOPHYSICAL RESEARCH LETTERS, VOL. 26, NO. 16, PAGES 2629-2632, AUGUST 15, 1999

Modulated electron-acoustic waves in auroral density cavities: FAST observations

R. Pottelette,[1] R. E. Ergun,[2] R. A. Treumann,[3,4] M. Berthomier,[1]
C. W. Carlson,[2] J. P. McFadden,[2] and I. Roth[2]

Abstract. We report on FAST observations of large amplitude (up to 500 mV m^{-1}) envelope solitary waves at the edges of the AKR source region. These edges are characterized by the presence of two electron populations: a dominant hot ($\sim$ keV) component and a minority cold ($<$ 60 eV) component. The nonlinear waves are recorded when the spacecraft passes the base of the parallel auroral acceleration region. They form intense packets of electron acoustic waves. The modulation is due to ion acoustic waves. These structures are electrostatic and propagate along the magnetic field at speeds of a few 100 km s^{-1}. They may play a crucial role in the acceleration processes taking place in these regions.

1. Introduction

Observations by the FAST satellite with orders of magnitude higher time and frequency resolution than provided by previous missions have detailed the density cavities that serve as the source regions of Auroral Kilometric Radiation (AKR) [*Ergun et al.*, 1998a; *Delory et al.*, 1998]. Measuring the electron number density in these regions is difficult, especially at low energies, where spacecraft photo-electrons often pollute the electron flux. Analysis of VLF wave measurements [*Strangeway et al.*, 1998] provided evidence for the hot ($>$ 1 keV) electrons to be the dominant electron component in these regions.

Here we show that the boundaries of the plasma cavities exhibit signatures of electron acoustic wave activity. Electron acoustic waves are known to contribute most to electrostatic high frequency noise excited in a two-component electron plasma when the density of the cold population is small compared to the density of the hot electrons [*Tokar and Gary*, 1984]. These conditions are given at the edges of the cavity where cold and hot electron densities mix. Under conditions of strong excitation and in the absence of simultaneously excited ion acoustic waves, the electron acoustic waves readily evolve into electron acoustic solitons which propagate at a speed faster than the electron acoustic velocity $v_{ea} = v_h\sqrt{n_c/n_h}$, which is the hot electron thermal velocity v_h multiplied by the root of the cold (n_c) to hot (n_h) electron density ratio. *Dubouloz et al.* [1991b, 1993] have demonstrated that electron acoustic solitary waves induce a broadband turbulent electric noise spectrum which exhibits a maximum in the neighbourhood of the cold plasma frequency. It is an ideal indicator of the presence of a cold electron component.

Electron acoustic waves like Langmuir waves are high frequency density waves. They may become trapped and modulated by ion acoustic density perturbations, leading to modulation and generation of electron acoustic envelope solitons [see e.g., *Dubouloz et al.,* 1991, 1993]. As we are going to demonstrate below, in the high time resolution of the FAST observations this kind of nonlinear structures are observed at the base of the parallel acceleration region each time the spacecraft enters into the upward ion acceleration region.

2. Observations

Figure 1 collects a sequence of wave and particle data recorded during the passage of the FAST satellite through the AKR source region on January 30, 1997 at $\sim$ 22 MLT (orbit 1750). The spacecraft was at an invariant latitude of $\sim 68^\circ$ and was travelling poleward - near apogee - at an altitude of 4300 km. The event shown took place in the upward current region. Figures 1a and 1b give the electric power spectral densities at high (4 kHz to $\sim$ 600 kHz) and low frequencies (32 Hz to 16 kHz), respectively. Figures 1c and 1d display the respective omnidirectional ion and electron energy fluxes versus energy and time for the same time period. Electron pitch-angle distributions at two different times are given in Figures 1e and 1f.

The FAST satellite entered the AKR source region at about 06:16:33 UT when auroral ion acceleration caused the sudden increase in the energy of the upgoing ions visible in Fig. 1c. Subsequently the satellite stayed for $\sim$ 24 s inside the AKR source region as is obvious from Figure 1a. This figure shows the presence of electromagnetic AKR emission generated at (and also slightly below) the local electron gyrofrequency f_{ce} at about 340 kHz (which is the dark line in the figure). The electron fluxes below 60 eV at this entire time period were polluted by spacecraft photo-electrons. At higher energies the whole region showed the presence of $\sim$ 5 to $\sim$ 20 keV precipitating electrons throughout the AKR source, while the equatorial and polar borders of the source region which were crossed at 06:16:32 UT and at 06 :16 :57 UT, respectively, indicated the presence of large numbers of electrons at perpendicular pitch angles with well expressed peak fluxes at 90° and 270° (Figure 1f).

Upgoing ion beams of energies approaching 10 keV in the center of the AKR source (Figure 1c) have also been detected. The ion pitch angle distributions show no evidence for neither downgoing nor a detectable low energy ion component. The entirety of these observations is consistent with the spacecraft passing two regions of parallel potential drops above and below its orbit.

[1]CETP, 4 avenue de Neptune, Saint-Maur des Fosses, France.
[2]Space Science Laboratory, UCB, Berkeley, California.
[3]MPE, Garching, Germany.
[4]ISSI, Bern, Switzerland.

Copyright 1999 by the American Geophysical Union.

Paper number 1999GL900462.
0094-8276/99/1999GL900462$05.00

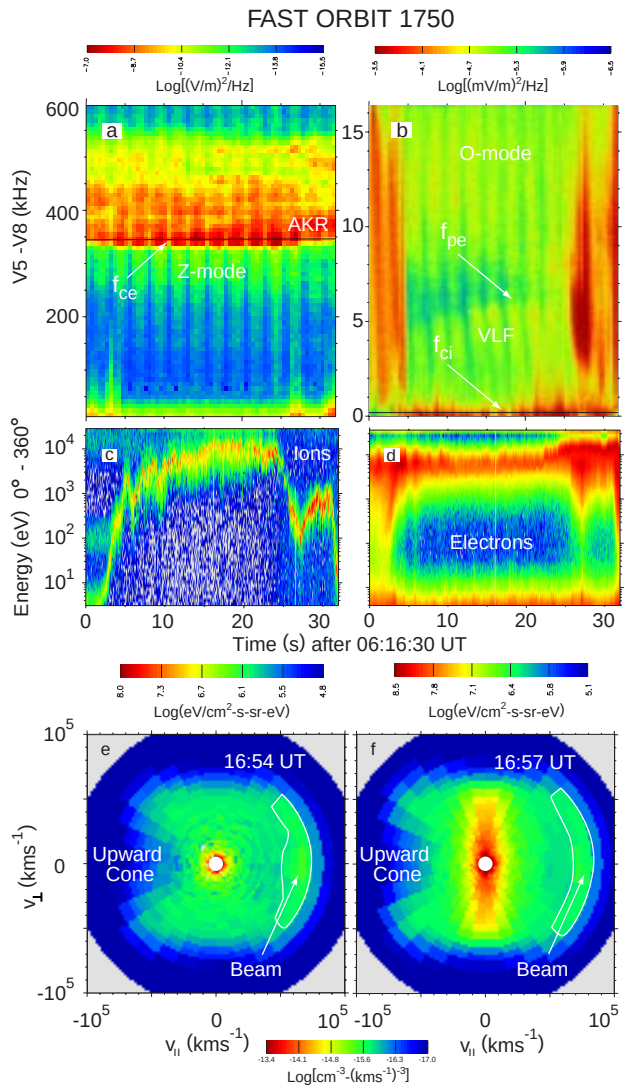

Figure 1. Fast wave and particle data in auroral density cavity. (*a*): HF wave spectrogram showing transversely polarized AKR emission at f_{ce} (dark line at $\sim$ 340 kHz) in X and below in Z mode and VLF waves. (*b*): VLF wave spectrogram showing parallel polarized O mode, electron acoustic and ion cyclotron (dark line at $\sim$ 200 Hz) waves. At base of AKR source broadband electron acoustic waves appear. (*c*): Ion and (*d*): electron energy spectra for same time interval. (*e*) and (*f*): Electron pitch-angle distributions in cavity and at base of AKR source with empty upward cone ($v_{\|} < 0$), fast (conical) electron beam ($v_{\|} > 0$), and hot electrons. Note the strong perpendicular heating of the latter (*f*) around 16:57 UT at the base. The white circle centered at $v = 0$ excludes the photo electrons.

Two wave modes above $\sim$ 1 kHz were recorded in the source region, as seen from Fig. 1b which is a blow-up of the lowest frequency part of Fig. 1a. Inspecting Fig. 1a, one observes that the spin modulations of the AKR, which is in the X-mode, and the low frequency waves are anticorrelated. Hence the low frequency modes of Fig. 1b have their electric fields polarized along the magnetic field. The mode in the lowest frequency range has a well defined upper frequency cutoff which during the passage of the spacecraft increases gradually from $\sim$ 4.5 kHz up to $\sim$ 5.5 kHz. This frequency range matches almost perfectly the plasma frequency of the hot electron ($\sim$ 60 eV) population whose density was measured by the electrostatic analyzers to be $n_h \approx 0.3$ cm^{-3}. This mode can be identified with the natural Langmuir wave. Its cutoff is the local plasma frequency. The nearly invariable maximum near $\simeq$ 12 kHz belongs to the second mode. This mode has a significant magnetic component. Consequently it is not locally generated. Rather it is the electromagnetic O-mode which is cut off at the total plasma frequency. These results confirm those previously obtained by *Strangeway et al.* [1998]. They show that although the presence of photoelectrons may induce spurious signals, the density of the hot electrons can be inferred from the properties of the VLF waves. Inside the AKR source region this energetic population dominates.

We now turn to the observation of intense broadband noise emissions which occur at the time when perpendicularly heated energetic electrons appear at the equatorial and polar edges of the AKR source region. These events took place around 06:16:32 UT and 06:16:57 UT (cf. Fig. 1). The broadband noise was lacking any measurable AC magnetic field signal. Thus it is almost electrostatic. In the following we concentrate on the event at 06:16:57 UT when the spacecraft arrived at the base of the parallel acceleration region, as indicated by the sudden drop of the ion beam energy from$\sim$ 6 keV to $\sim$ 100 eV (see Fig. 1c).

The left part of Fig. 2 displays 20 ms of data covering this event. In the right part of Fig. 2 we show the spectrum of these waves taken over 300 ms, when the electric antenna was parallel to the magnetic field. The electric field signal was dominated by a series of large amplitude, strongly modulated coherent wave packets which were spatially periodic and had a recurrence period of $\sim$3 ms corresponding to waves of frequency $\sim$300 Hz, well in the hydrogen ion acoustic frequency range. Note the strong localization of the wave packets in time and space and their separation by gaps of nearly vanishing wave amplitude. Also note the strong monochromaticity of the high frequency waves trapped wave in the localized wave packets as indicated by the intense $\simeq$5 kHz peak in the spectrum at the right. Measurements performed by the two orthogonal electric antennae suggest that the wave field was directed almost perfectly parallel to the magnetic field. The 5 kHz emission line can be interpreted as the cold electron plasma frequency yielding a cold number density of $\sim 0.3\,\mathrm{cm}^{-3}$. During this event the hot ($>$ 60 eV) electron density peaks near $\sim 1.5\,\mathrm{cm}^{-3}$. Hence, the secondary much frequency weaker emission at $\simeq$ 12 kHz matches the value of the total plasma frequency.

3. Discussion and Conclusions

In order to infer about the excitation mechanisms of the dominant wave modes, viz. the electron acoustic and ion acoustic waves, we recall that from Fig. 1c-1f four different particle populations can be identified at the edge of the AKR source region. The first is the downward directed anisotropic energetic auroral electron beam (or electron conic) near $15-25$ keV. This beam is fast, $v_b \simeq 6\times10^4$ km s^{-1}, and relatively dense, $n_b \simeq 0.024$ cm $^{-3}$, which is about 0.1% of the total plasma density. Its parallel and perpendicular temperatures are $T_{b\|} \approx 1$ keV, $T_{b\perp} \approx 3$ keV. Its distribution peaks parallel to the magnetic field. Hence, it is responsible for the excitation of the Langmuir wave spectrum at the total

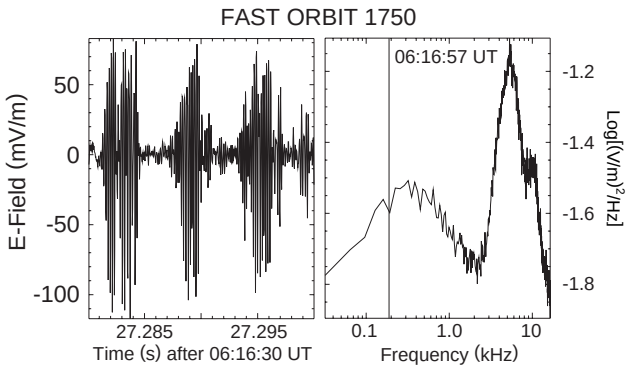

Figure 2. *Left*: Wave form of broadband noise at base of AKR source. The signal consists of highly coherent (nearly monochromatic frequency of trapped wave) wave packets. *Right*: Frequency spectrum of broadband noise showing the electron acoustic wave (at $\sim$ 5 kHz) and total plasma frequency (at $\sim$ 12 kHz) peaks. The broad LF maximum near 300 Hz belongs to the ion acoustic wave spectrum participating in the 3 ms modulation of the electron acoustic waves.

plasma frequency. Probably it is also involved in excitation of other high-frequency modes and in AKR.

In addition to the electron beam one has the hot auroral electron component with temperatures comparable to the beam, and a dilute ($n_c/n_h \approx 20\%$) cold electron component, as well as the energetic but relatively cool upward ion beam. Since we are definitely in the region of a nonvanishing parallel electric field and upward currents there is no need for total electric charge compensation. The hot and cold electron components are moving downward though at substantially different velocities, $v_{Dh} \simeq 200 - 300$ km s^{-1}, $v_{Dc} < v_{Dh}$. The latter velocity is not possible to determine from the measurements. The ion beam, on the other hand, propagates upward at speed of about $v_{bi} \sim 100$ km s^{-1}, which is substantially lower than in the center of the electron density trough, while the temperature of the ions, taken from the spread of the distribution function in Fig. 1c, is also decreased at the bottom of the acceleration region. There are no cold background ions above detectability of the instrumentation.

Except for the auroral electron beam, the three particle components provide the free energy and the propagation conditions for waves. Figure 3 shows a sketch of their distribution functions. In the frame of the cold slowly drifting electron distribution the hot auroral electrons form a broad distribution centered at $v_{Dh} > v_{Dc}$. This is equivalent to the case of an ion acoustic instability (the electron acoustic instability is the analogue to the ion acoustic instability with the only difference that it suffers stronger damping because of the easier mobility of the cold electrons than the ions in the former). Under these conditions electron acoustic waves become unstable. For instability a very dilute cold electron population is needed [*Tokar and Gary*, 1984]. The physical reason is that for nonnumerous cold electrons the damping of the electron acoustic waves is strongly reduced while the cold electron component allows the waves to propagate. This condition is satisfied here, with the waves propagating on the cold electron background while riding on the hot with wave speed $v_c < v_{ea} < v_{Dh}$ which requires $v_{Dh} > v_c$. In analogy to the ion acoustic case, the latter condition for instability is not very restrictive as the grainedness of the electron phase space causes electron holes to evolve in the bulk of the hot beam as evidenced by *Ergun et al.* [1998b]. They lower the instability threshold supporting the generation of a broad spectrum of electron acoustic waves. Using the $\sim$ 1 keV parallel electron temperature of the hot component one finds a typical wavelength of electron acoustic waves of $\lambda_{ea} \sim 1$ km.

The excitation of ion acoustic waves can be understood when neglecting the cold electrons. Ion acoustic waves propagate on the ion component. They are thus carried by the ion beam. The condition for instability is that $v_{Dh} > c_{ia} = v_h\sqrt{m_e/m_i}$. Since the ion beam is upward propagating in the opposite direction of the hot electrons this condition is easily satisfied (see Fig. 3). The waves are excited in a broad range of phase velocities below the hot electron component drift velocity $2\pi f_{ia}/k < v_{Dh}$. These waves can be excited up to the ion plasma frequency, which yields for their wave number cut-off $k_{ia} < 2\pi f_{pi}/v_{Dh}$. The typical wavelength of these waves is of the order of $\lambda_{ia} \sim \lambda_{ea}$. In the cold electron frame these waves move upward with the ion beam. In the fixed system of the Earth, however, they move downward together with the higher frequency electron acoustic waves because their phase velocity is so close to v_{Dh}. We therefore end up with a situation where all the electrostatic waves are essentially moving down. In such a scenario the ion acoustic waves can both modulate and trap electron acoustic waves to generate wave packets similar to the observed packets. Trapping is in principle possible up to any multiple half of the electron acoustic wavelength.

The discussion shows that obviously the data support the view that a pre-existing field-aligned potential is the ultimate cause of the excitation of the observed wave spectra. However, their nonlinear evolution and modulation may also contribute to secondary generation of localized fields and further acceleration. It is interesting to investigate the pon-

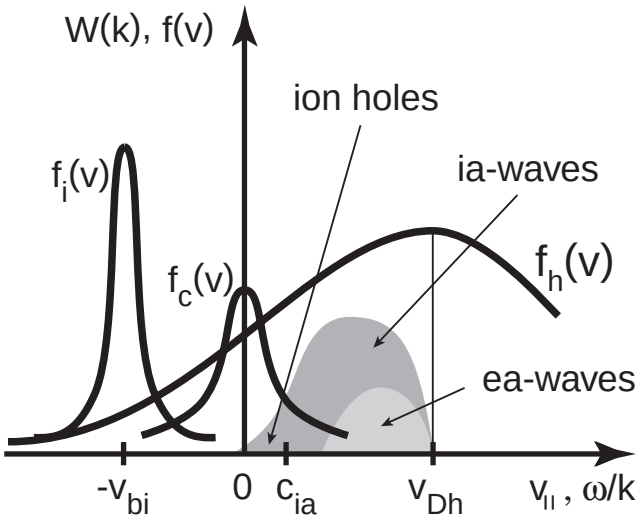

Figure 3. Sketch of the particle distribution functions $f(v)$ leaving out the auroral electron beam. Unstable spectra $W(k)$ of electron and ion acoustic waves as function of wave phase speed ω/k are indicated by shading. Both types of waves move downward in the cold electron and ion frames.

deromotive force acceleration of cold electrons [*Pottelette et al.*, 1993] in the resulting envelope solitons. The ponderomotive force potential can be calculated from the nonlinear term in the particle (fluid) equation [*Treumann and Baumjohann*, 1996]. When the high frequency field is identified with the electron acoustic wave field, the electric potential for electrons assumes the form $\Delta\phi_{\parallel} \approx (\epsilon_0/4en_c)E_{\parallel}^2$. Taking the observed values of $E_{\parallel} \sim 200\,\mathrm{mV\,m^{-1}}$ and $n_c \sim 0.3\,\mathrm{cm^{-3}}$, the energy that the cold electrons can get interacting in the parallel direction with one electron acoustic soliton amounts to ~ 2 eV. This may look as a rather weak value. However, interaction with many solitons may lead to substantial acceleration. Electric potential drops may also result from the spatial arrangement of many microscopic solitary structures, when every elementary potential drop contained in each single soliton adds up along the field line over mesoscale distances as proposed by *Pottelette et al.* [1993] and *Ergun et al.* [1998b].

The above results have been confirmed for other FAST orbits as well. In short, from wave observations we have inferred that: (1) electron acoustic waves are generated at the edges of the AKR source density cavity; (2) these observations enable us to determine the density fraction n_c/n_h; (3) modulated electron acoustic solitons are recorded each time the spacecraft enters the base of the parallel acceleration region; (4) the waves have typical parallel scales of ~ 1 km and are moving downward at a velocity of a few hundred $\mathrm{km\,s^{-1}}$; (5) the waves are the ultimate result of a parallel electric field in the upward auroral current region, they may, however, themselves self-consistently contribute to the generation of such large-scale parallel electric fields.

Acknowledgments. This research has been initiated within the France-Berkeley Program. Part of the work was supported by the PROCOPE cooperation under contract number D/9822921. We thank the two referees for their constructive comments.

References

Delory, G. T., R. E. Ergun, C. W. Carlson, L. Muschietti, C. C. Chaston, W. Peria, J. P. McFadden, and R. Strangeway, FAST observations of electron distributions within AKR source regions, *Geophys. Res. Lett., 25*, 2069-2072, 1998.

Dubouloz, N., R. Pottelette, M. Malingre, and R. A. Treumann, Generation of broadband noise by electron acoustic solitons, *Geophys. Res. Lett., 18*, 155-158, 1991.

Dubouloz, N., R. A. Treumann, and R. Pottelette, Turbulence generated by a gas of electron-acoustic solitons, *J. Geophys. Res., 98*, 17415-17422, 1993.

Ergun, R. E. *et al.*, FAST satellite wave observations in the AKR source region, *Geophys. Res. Lett., 25*, 2061-2064, 1998a.

Ergun, R. E. *et al.*, FAST satellite observations of large amplitude solitary structures, *Geophys. Res. Lett., 25*, 2061-2064, 1998b.

Pottelette, R., M. Malingre, A. Bahnsen, L. Eliasson, K. Stasiewicz, R. E. Erlandson, and G. Marklund, Viking observations of bursts of intense broadband noise in the source region of auroral kilometric radiation, *Ann. Geophys.*, *6*, 573-586, 1988.

Pottelette, R., M. Malingre, N. Dubouloz, B. Aparicio, R. Lundin, G. Holmgren, and G. Marklund, High-frequency waves in the cusp/cleft regions, *J. Geophys. Res., 95*, 5957-5971, 1990.

Pottelette, R., R. A. Treumann, G. Holmgren, N. Dubouloz, and M. Malingre, Acceleration and radiation from auroral cavitons, in *Auroral Plasma Dynamics*, edited by R. L. Lysak, pp. 253-265, AGU, Geophys. Monograph 80, Washington, D. C., 1993.

Strangeway, R. J. *et al.*, FAST observations of VLF waves in the auroral zone: Evidence of very low plasma densities, *Geophys. Res. Lett., 25*, 2065-2068, 1998.

Tokar, R. L. and S. P. Gary, Electrostatic hiss and the beam driven electron acoustic instability in the dayside polar cusp, *Geophys. Res. Lett., 11*, 1180-1183, 1984.

Treumann, R. A. and W. Baumjohann, *Advanced Space Plasma Physics*, 381 pp., Imperial College Press, London, 1997.

M. Berthomier and R. Pottelette CETP, 4 avenue de Neptune, F-94107 Saint Maur des Fosses, France. (e-mail: pottelet@cetp.ipsl.fr)

C. W. Carlson, R. E. Ergun, J. P. McFadden, and I. Roth, Space Sciences Laboratory, University of California, Berkeley, CA 94720. (e-mail: ree@ssl.berkeley.edu)

R. A. Treumann, Max-Planck-Institute for extraterrestrial Physics, POBox 1603, D-85740 Garching, Germany, and International Space Science Institute, Hallerstr. 6, CH-3012 Bern, Switzerland. (e-mail: tre@mpe.mpg.de)

(Received March 18, 1999; accepted May 6, 1999.)